

# Monocyclic $\beta$ -Lactams Are Selective, Mechanism-Based Inhibitors of Rhomboid Intramembrane Proteases

Olivier A. Pierrat,<sup>†,§</sup> Kvido Strisovsky,<sup>†,§</sup> Yonka Christova,<sup>†</sup> Jonathan Large,<sup>‡</sup> Keith Ansell,<sup>‡</sup> Nathalie Bouloc,<sup>‡</sup> Ela Smiljanic,<sup>‡</sup> and Matthew Freeman<sup>†,\*</sup>

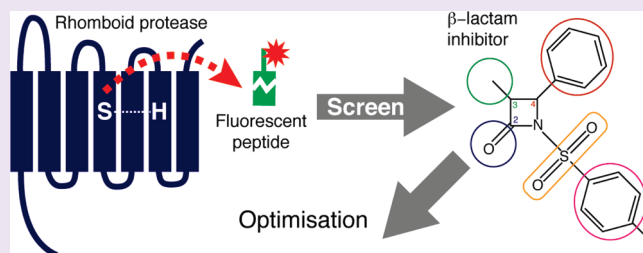
<sup>†</sup>MRC Laboratory of Molecular Biology, Hills Road, Cambridge CB2 0QH, U.K.

<sup>‡</sup>Centre for Therapeutics Discovery, MRC Technology, 1-3 Burtonhole Lane, Mill Hill, London NW7 1AD, U.K.

**S** Supporting Information

**ABSTRACT:** Rhomboids are relatively recently discovered intramembrane serine proteases that are conserved throughout evolution. They have a wide range of biological functions, and there is also much speculation about their potential medical relevance. Although rhomboids are weakly inhibited by some broad-spectrum serine protease inhibitors, no potent and specific inhibitors have been identified for these enzymes, which are mechanistically distinct from and evolutionarily unrelated to the classical soluble serine proteases.

Here we report a new biochemical assay for rhomboid function based on the use of quenched fluorescent substrate peptides. We have developed this assay into a high-throughput format and have undertaken an inhibitor and activator screen of approximately 58,000 small molecules. This has led to the identification of a new class of rhomboid inhibitors, a series of monocyclic  $\beta$ -lactams, which are more potent than any previous inhibitor. They show selectivity, both for rhomboids over the soluble serine protease chymotrypsin and also, importantly, between different rhomboids; they can inhibit mammalian as well as bacterial rhomboids; and they are effective both *in vitro* and *in vivo*. These compounds represent important templates for further inhibitor development, which could have an impact both on biological understanding of rhomboid function and potential future drug development.



Intramembrane proteases are relative newcomers to the long list of proteases that control many biologically and medically important cellular processes. The four families of intramembrane proteases comprise site-2 protease,<sup>1</sup> presenilin/ $\gamma$ -secretase,<sup>2</sup> signal peptide peptidase,<sup>3</sup> and rhomboids.<sup>4</sup> The last are intramembrane serine proteases but, like all the other families, are evolutionarily unrelated to their well-known soluble counterparts. Rhomboids exist in most sequenced organisms and, despite ignorance of many of their functions, are already known to participate in processes as diverse as growth factor signaling,<sup>4–6</sup> mitochondrial function,<sup>7–9</sup> invasion of host cells by apicomplexan parasites,<sup>10–12</sup> and bacterial protein export.<sup>13</sup>

One of the key differences between rhomboids and other serine proteases is that their active site resides in the lipid bilayer of membranes, where it is formed by residues contributed by transmembrane helices.<sup>4,14</sup> This characteristic membrane environment establishes biophysical constraints on any potential inhibitors and also raises questions about the potential *in vivo* availability of inhibitors that might work *in vitro* in a detergent micelle system. There are no selective inhibitors yet reported for any rhomboids, although they are (weakly) inhibited by isocoumarins, broad-spectrum inhibitors of serine proteases, and a few other serine protease inhibitors.<sup>4,15</sup>

There are strong incentives to identify selective rhomboid inhibitors. As research tools, such inhibitors could dramatically accelerate progress in discovery of the physiological role of

rhomboids, especially in higher organisms such as mammals, where a genetic approach is slow and difficult. Furthermore, although they are not yet fully validated disease targets, there are very strong indications that rhomboid inhibitors are likely to have medical utility.<sup>10,12,16–18</sup> Being proteolytic enzymes, it seems likely that rhomboids are inherently amenable to small molecule inhibitor screening.

Here we describe the development of a new *in vitro* assay of rhomboid activity based on the use of fluorogenic peptides that span the recognition motif and cleavage site of known substrates. We have further developed this assay into a high-throughput format and undertaken a screen of a library of small molecules to look for compounds that can inhibit (or activate) rhomboid activity. This approach has led to the identification of a series of monocyclic  $\beta$ -lactams, the first potent and selective rhomboid inhibitors.

## RESULTS AND DISCUSSION

**Development of an *in Vitro* HTS Rhomboid assay.** Previously reported *in vitro* assays of rhomboid activity have relied on incubating detergent-solubilized rhomboids with radioactive

**Received:** October 8, 2010

**Accepted:** December 22, 2010

**Published:** December 22, 2010

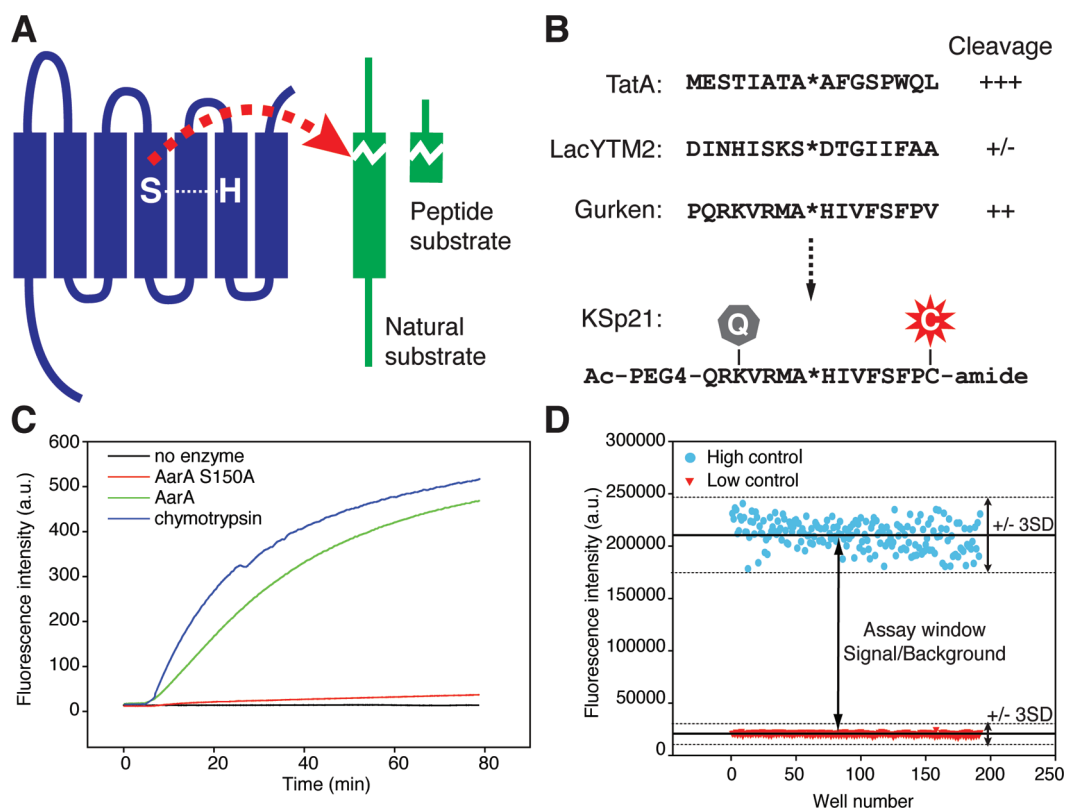


**Figure 1.** Fluorescent assay design. (A) Schematic representation of rhomboid enzyme AarA cleaving a natural rhomboid substrate or a substrate-based peptide. (B) Comparison of AarA activity on three peptides derived from known rhomboid substrates. Rhomboid cleavage sites (asterisks) were determined by HPLC using peptide standards or MALDI-TOF mass spectrometry. The Gurken-derived peptide was modified with QSY21 dark quencher and Chromis-645 fluorophore to yield fluorogenic peptide KSp21. (C) Time course of cleavage of  $1 \mu\text{M}$  KSp21 by  $0.4 \mu\text{M}$  AarA (wt or S150A) or  $0.2 \mu\text{M}$  chymotrypsin, at  $25^\circ\text{C}$ . (D) Fluorescent activity assay adapted to high-throughput screen (HTS) format.  $Z'$  factor = 0.77 (signal/background = 10, coefficients of variation = 6%) (see Methods). High control = AarA + DMSO; low control = no enzyme + DMSO.

or non-radioactive protein substrates that encompassed the full transmembrane domain (TMD) and flanking regions.<sup>15,19–21</sup> These approaches were not readily adaptable to a high-throughput screening (HTS) format, so we investigated the possibility of generating suitable fluorogenic peptidic substrates for rhomboids. Although natural substrates are full-length TMDs, rhomboids typically rely on a short recognition motif to determine cleavage.<sup>19</sup> We therefore tested the ability of short peptides derived from known rhomboid substrates to be cleaved by purified bacterial rhomboid proteases *in vitro* (Figure 1A,B). HPLC and mass spectrometry analysis showed that synthetic peptides derived from *Providencia stuartii* TatA and *Drosophila* Gurken were cleaved by *P. stuartii* and *E. coli* rhomboids AarA and GlpG at their natural cleavage sites,<sup>19</sup> albeit with varying efficiencies (Figure 1B).

The ability of rhomboids to cleave short peptides allowed us to develop fluorogenic peptide substrates, suitable for high-throughput screening. We introduced several Förster resonance energy transfer (FRET) donor–acceptor pairs into the TatA and Gurken peptides, modifying residues that had been shown not to be part of the recognition motif of the substrate.<sup>19</sup> We tested a range of fluorescent dyes (MCA, TAMRA-550, AlexaFluor-647, Chromis-645), and the best results were obtained with a Gurken-derived 15-mer peptide, labeled by the Chromis-645/QSY21 FRET pair at the C-terminus and P5 position, respectively (Figure 1B). This peptide, KSp21, had better aqueous solubility than the other FRET-labeled peptides and was the most efficient

fluorogenic substrate for AarA, the rhomboid whose substrate specificity is best understood. Progress curves of KSp21 cleavage by AarA, recorded continuously, were exponential, with a linear initial phase (Figure 1C). The initial reaction rate increased linearly with enzyme concentration up to  $200 \text{ nM}$  (Figure S1A) and to substrate concentration up to  $1 \mu\text{M}$  (data not shown). At higher substrate concentrations ( $>2 \mu\text{M}$ ), KSp21 precipitated, which prevented us from determining its apparent  $K_M$  and  $V_{max}$ . The solubility of KSp21 was improved by increasing DMSO concentration in the assay buffer, which also enhanced AarA activity. In a miniaturized format ( $20 \mu\text{L}$ , 384-well plate) adapted to HTS, the assay showed an excellent robustness with  $Z'$  score (statistical indicator of assay reproducibility and sensitivity<sup>22</sup>) of  $\sim 0.8$  and a large assay window (Figure 1D). We concluded that the KSp21-based fluorescent assay, using the rhomboid AarA, provided an effective platform for a high-throughput screen for rhomboid inhibitors and activators.

**A High-Throughput Screen.** A flowchart summarizing the different steps of the screening campaign is illustrated in Figure 2A.

**Pilot and Full Screens.** The KSp21-based assay was validated in a pilot screen of the NINDS collection of 1,040 bioactive compounds (ICCB Longwood, Harvard Medical School). We obtained  $Z'$  and  $Z$  ( $Z$ , the ratio of separation band to the signal dynamic range, allows the comparison between HTS assays<sup>22</sup>) factors of 0.9 and 0.6–0.8, respectively, and a correlation between two runs of  $R^2 = 0.79$ , with a hit rate of 2.6% (cutoff

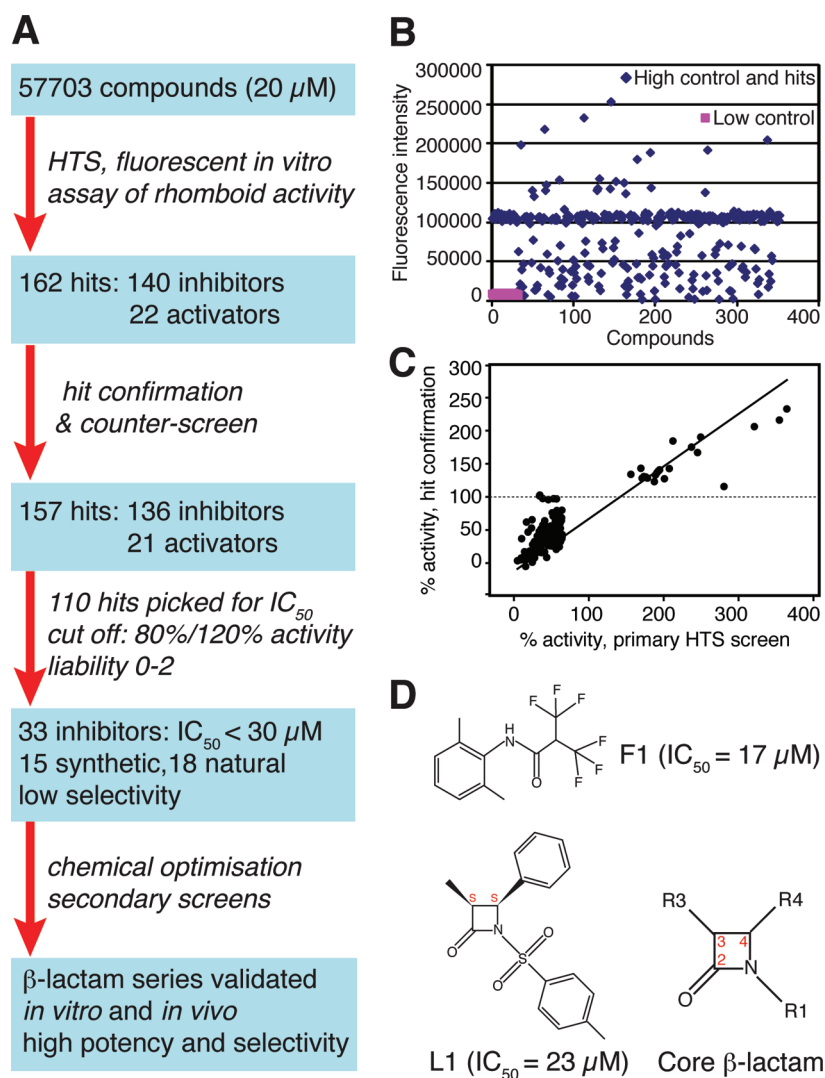


**Figure 2.** Screening campaign summary. (A) Screen flowchart. (B) Fluorescent signal of 162 initial hits and 190 high controls (DMSO + AarA), both denoted by blue diamonds, and 32 low controls (DMSO, no enzyme), denoted by magenta squares. DMSO high controls or inactive compounds cluster around the 100,000 activity units mark, inhibitors are represented by points below 100,000 activity units, and activators are above. (C) Plot of correlation between initial hits from high-throughput screen and secondary screen; 7 hits (6 false inhibitors, 1 false activator) were not confirmed as they showed  $\sim 100\%$  activity in the second screen (dotted line). (D) Chemical structure and apparent  $\text{IC}_{50}$  values of hits selected for chemistry optimization: series 1, bis(trifluoromethyl)-amide (bis- $\text{CF}_3$ ), based on compound F1; and series 2, monocyclic  $\beta$ -lactam, based on compound L1.

as defined in Methods). These statistics strongly validated the technical quality of the screen.<sup>22</sup> We therefore ran a full primary screen for inhibitors and activators of AarA from a library of 57,703 molecules, comprising a set of diverse compounds from a variety of commercial suppliers, two small libraries of protease and kinase inhibitors, and a collection of 2,000 natural compounds (Analyticon). Compounds were screened at 20  $\mu\text{M}$ , and AarA activity was measured by reading fluorescence after stopping the reaction. The statistics of the screen were comparable to the pilot ( $Z' = 0.7-0.9$ ), but hit rates were lower: 0.1–0.2% (synthetic molecules from the diversity set and focused libraries) and 1.3% (natural compounds). Interestingly, the 53 compounds of the Biomol classic protease inhibitors set (Enzo Life Sciences) did not give any hits, except the broad range serine protease inhibitor dichloroisocoumarin (DCI), a known rhomboid inhibitor. Combined with previous data that most serine protease inhibitors do not affect rhomboids,<sup>4,15</sup> this illustrates that rhomboids are indeed novel targets.

**Hit Confirmation and Counter-screen.** We picked 162 compounds from the full screen and confirmed 97% of them in the same fluorescent assay (Figure 2B,C). In a counter-screen, the compounds were added postreaction to identify any false positives that interfere with the assay technology itself (e.g., precipitation-inducers, quenchers, or fluorescent compounds). No interfering compounds were detected, but one false activator was discarded (data not shown).

**$\text{IC}_{50}/\text{EC}_{50}$  Measurements and Hit Ranking.** A subset of 110 hits that inhibited AarA activity to less than 80% or increased it to more than 120% of the control and showed liability of 0 to 2 (defined as the frequency that the same compound has been hit in 16 previous screens of the same library against unrelated enzymes, thus excluding any obviously promiscuous and unspecific effectors), were characterized further. The potency of these compounds, including both inhibitors and activators, was determined by titrating their effect on AarA activity in the fluorescent assay. Subsequent kinetics revealed that the best activators were

rather weak ( $EC_{50} > 0.1$  mM), although they did produce up to 30-fold increase in initial rate at the highest concentration tested (100  $\mu$ M; data not shown). Despite their potential interest, these activators were not pursued further in this study.

Continuous recording of reaction time courses was used to rank inhibitors by potency and selectivity over chymotrypsin, an unrelated serine protease. After plotting the initial rate of reaction versus compound concentration, we used a 4-parameter logistic equation to fit our data (Sigma Plot 11, Systat Software, Inc.) and calculate the apparent  $IC_{50}$  values (for simplicity,  $IC_{50}$  henceforth). We defined the rhomboid selectivity as the ratio of  $IC_{50}$  against chymotrypsin: $IC_{50}$  against AarA. Of the 33 inhibitors with  $IC_{50}$  lower than 30  $\mu$ M, 15 were synthetic small molecules (S1–S15, Table S1a) and 18 were natural products or semisynthetic analogues thereof (N1–N18, Table S1b). The natural products were highly heterogeneous in structure and not amenable to chemical optimization or rapid analogue synthesis and so were not pursued further. The synthetic compounds showed more promise. Strikingly, five related bis(trifluoromethyl) amide compounds (“bis- $CF_3$ ”, prefixed “F”, Table S1a and Figure 2D) formed a distinctive series of inhibitors with a best  $IC_{50} \leq 20$   $\mu$ M. Despite their low liability, these initial hits also inhibited chymotrypsin (selectivity 0.5–1). We also chose to pursue the monocyclic  $\beta$ -lactam S12/L1 ( $\beta$ -lactam series prefixed “L”, Figure 2D) which, despite being slightly less potent ( $IC_{50} = 23$   $\mu$ M) than the bis- $CF_3$  compounds, had other encouraging attributes. Despite inhibiting chymotrypsin (selectivity 0.7), L1 had a liability of zero and, apart from cephaloridine (a broad spectrum antibiotic with cytotoxicity; promiscuous, with liability  $>2$  in our screen), was uniquely positive among 87 other  $\beta$ -lactams in the library (not shown). Furthermore, the  $\beta$ -lactam motif present in L1 is a commonly occurring substructure within the protease inhibitor field, and several are well established as drugs. No other hits survived the triage process or brief exploratory chemistry to be selected for further analysis.

**Structure–Activity Relationships and Selectivity of Hit Analogues.** In the previous section, we described the selection of two classes of hit from the primary screen for optimization by chemical modification: the bis- $CF_3$  compounds (F1–F5) and the monocyclic  $\beta$ -lactam L1. Each was used as a starting point for the chemical synthesis of related compounds, which were then assayed for potency and selectivity against AarA using the fluorescent peptide assay. Subsequently, active hits were validated in an independent *in vitro* assay, using a whole membrane protein substrate instead of a fluorescent peptide, and tested for selectivity against a different rhomboid showing similar substrate specificity, *E. coli* GlpG.<sup>19</sup>

**Bis- $CF_3$  Compounds (F-Series).** A total of 108 chemical structures related to compound F1 were either purchased or synthesized (structures and detailed results in Table S2). Modification or replacement of the bis(trifluoromethyl) group was attempted in the following ways: steric replacement of the fluorine atoms (F6, F9–11, F18, F23), “acidity”/chemical modifications (F15, F17, F24–26) including sulfone (F16), classical protease warhead-type replacements (F8, F12–14, F22), and moving/deleting the fluorines (F4–5, F7, F19). All of these changes to the bis- $CF_3$  moiety completely destroyed inhibitory activity in the fluorescent assay. On the left-hand side of the molecule (Figure 2D), a range of substituents on the aniline ring were tolerated (Table S2), but replacement with a pyridine ring (F27–F29) was not. The best compounds were up to 17-fold more potent than F1, with  $IC_{50}$  values in the low micromolar

range (F70–F73, Figure 3A). Despite this improvement, the structure–activity relationship analysis (SAR) of the aniline portion was rather flat, although the degree of selectivity over chymotrypsin was significantly improved (Figure 3A, Table S2). A number of analogues showed a net preference for AarA over chymotrypsin; among them, compounds F61 and F102 combined good potency with excellent selectivity.

Despite this quite promising improvement of the bis- $CF_3$  compounds, when tested against a full-length substrate in the gel-based assay, they raised significant concerns. Even at low micromolar levels they triggered formation of high molecular weight protein complexes, combined with the disappearance of the GlpG (Figure 3B), suggesting that they may cause aggregation of both enzyme and substrate. Indeed, in the presence of bis- $CF_3$  compounds, substrate aggregated in the absence of enzyme, and enzyme oligomerized without substrate (data not shown). Although we have not investigated their mechanism of action and their low liability suggests that they might be acting more specifically than simply as unselective protein aggregators, these data were of sufficient concern to make us decide not to pursue this series further.

**$\beta$ -Lactams (L-Series).** A total of 58 analogues of  $\beta$ -lactam L1 were synthesized. Potency and specificity data of key compounds are shown in Table 1, and full details are in Supplementary Table S3; we here describe our main conclusions about structure–activity relationship of this series. As shown in Figure 2D, we introduced structural changes at all four positions on the  $\beta$ -lactam ring: the N-substituent (R1), the carbonyl group at C-2 and substituents at C-3 and C-4.

- Deletion of the C-2 carbonyl group (L30–31) suppressed activity, lending support to a mechanism-based mode of inhibition analogous to other  $\beta$ -lactam serine protease inhibitors, in which the rhomboid catalytic serine nucleophilically attacks the carbonyl group at C-2.
- As the N-sulfonyl substituent is predicted to make the  $\beta$ -lactam ring very reactive, we tested straight-chain analogues to see whether the ring-opened form was responsible for inhibition. The chloroketones TPCK and TLCK were inactive against AarA, as were analogues L36–40, implying that the intact  $\beta$ -lactam ring is required for inhibitory activity.
- Activity against AarA was suppressed by sulfonyl removal (L6–7) or replacement by urea (L28, L32–33), amide (L8, L12), or carbamate (L29). L34 was atypical as it retained activity against AarA despite the amide modification.
- An N-aryl sulfonyl substituent was essential (L9 inactive), and lipophilic *meta*-substituents improved potency (L19–20, L42, L44–45).
- Although the aryl ring at C-4 was not required for activity, its presence improved potency further, as did small lipophilic *meta*-substituents (L44–45). Up to 4-fold gain in potency against AarA was achieved in L44, by combining *meta*-substituents on both aryl rings.
- The methyl group at C-3 in L1 was not essential (L2, L4–5, L14, L16–20, L35, L41–49 and L58), but the parent (unsubstituted)  $\beta$ -lactam L15 was inactive. Amide derivatives at C-3 reduced (L50–54) or abolished activity (L55–57).

The  $\beta$ -lactams showed very different degrees of selectivity for rhomboids over chymotrypsin. Out of 58 compounds, 19 strongly preferred chymotrypsin, whereas 6 preferred AarA (L14, L25–26, L41–42 and L54). Three of these six compounds

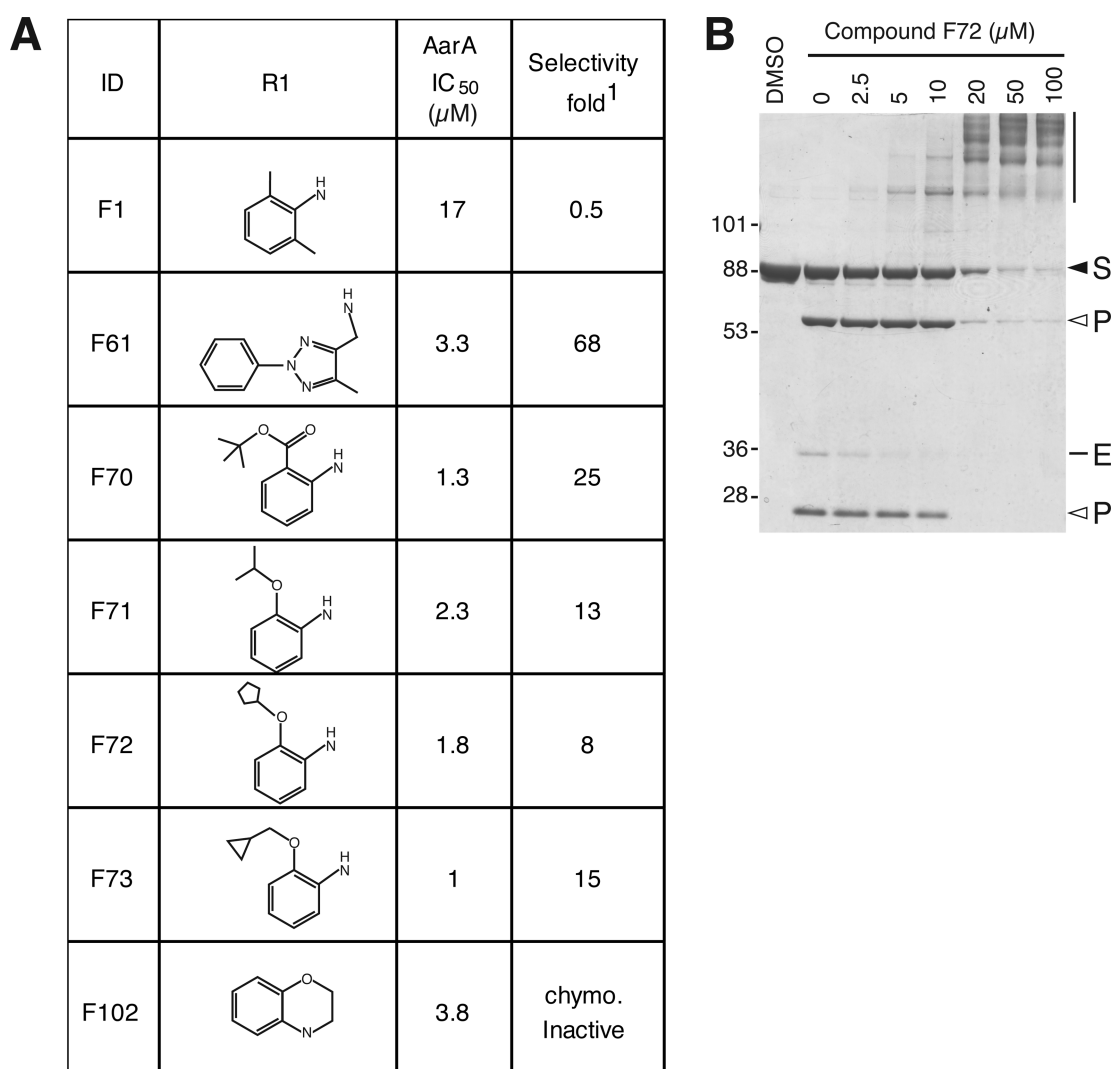


**Figure 3.** *In vitro* effects of selected bis-CF<sub>3</sub> analogues with modifications of the aniline moiety. (A) Results of fluorescent assay with 600 nM KSp21 peptide and either 100 nM AarA or 37 nM chymotrypsin. (B) Gel-based assay with 320 nM GlpG and 3  $\mu$ M Gurken chimeric substrate and increasing concentration ( $\mu$ M) of inhibitor F72. Enzyme (E) substrate (S), and product (P) bands are labeled on the right-hand side of the gel. High molecular weight protein aggregates appear (vertical line) as inhibitor concentration increases.

combined selectivity for AarA with high potency: L25 and L26, without a substituent at C-4 (inactive on chymotrypsin), and L42 containing a 3'-biaryl sulfonyl group. This potential for high selectivity in favor of rhomboids is important, as it contrasts with other known rhomboid inhibitors (of which isocoumarins are best characterized), which are broad-spectrum serine protease inhibitors.<sup>23</sup>

In conclusion, the potency of these  $\beta$ -lactams against AarA was significantly improved after chemical optimization, so that the best IC<sub>50</sub> values in the fluorescent assay were equivalent to that of DCI (L42, L44–45). Importantly, several  $\beta$ -lactams showed much better selectivity than DCI for rhomboid over chymotrypsin.

**$\beta$ -Lactams Show High Potency and Selectivity for GlpG.** Unlike the bis-CF<sub>3</sub> compounds, the  $\beta$ -lactams did not trigger substrate or enzyme aggregation in the gel-based assay of GlpG (Figure 4A) or AarA (data not shown), which relies on full-length protein substrates. Moreover, many showed high potency against GlpG (Figure 4B, Table 1), the best IC<sub>50</sub> values being around 0.4–0.8  $\mu$ M. We noted that IC<sub>50</sub> values against AarA were 2-fold (L58) to 14-fold (L44) higher (Table 1) in the assay based on

full-length proteins than in the fluorescent assay; in fact, L35 and L41 did not inhibit AarA at all in this assay, but they did in the fluorescent peptide assay. The greater resistance to inhibition in the full-length protein assay presumably reflects the different nature of the two assays, for example, concentration differences and the possibly higher affinity for the enzyme of a full-length, TMD-containing substrate, compared to a short peptide. We are unable to make a direct comparison of IC<sub>50</sub> values against GlpG in the two assays, as GlpG does not cleave the KSp21 fluorescent peptide.

SAR data show a clear relationship between compound structure and selectivity between the two rhomboids (Tables 1 and S3). For instance, certain substituents at C-4 lead to a complete preference for AarA (L14, L44, and L46) over GlpG. Similarly, L26 inhibited only AarA, in contrast with L25. On the other hand, GlpG was preferably targeted if the *N*-sulfonyl substituent was replaced (e.g., L8, L29), suggesting that GlpG could tolerate greater structural changes at this position. Curiously, the re-synthesized racemic 3,4-*cis*-L1 (relative *cis* C-3:C-4 stereochemistry) was very potent on GlpG, whereas only the single enantiomer 3*S*,4*S*-L1 (HTS hit) was active on AarA. Many  $\beta$ -lactams

Table 1. Structure–activity Relationship of Key  $\beta$ -Lactam Compounds Described in the Main Text

ID	Structure	Enzyme	<i>In vitro</i> fluorescent assay IC <sub>50</sub> ( $\mu$ M)	<i>In vitro</i> gel-based assay IC <sub>50</sub> ( $\mu$ M)	<i>In vivo</i> <sup>1</sup> EC <sub>50</sub> ( $\mu$ M)	ID	Structure	Enzyme	<i>In vitro</i> fluorescent assay IC <sub>50</sub> ( $\mu$ M)	<i>In vitro</i> gel-based assay IC <sub>50</sub> ( $\mu$ M)	<i>In vivo</i> <sup>1</sup> EC <sub>50</sub> ( $\mu$ M)	
L1 (S)		AarA	30	nd		L26		AarA	26	nd*		
		chymo	21	na				chymo	inactive	na		
AarA		inactive	inactive	GlpG				na	inactive			
L1 (rac.)			chymo	1.6		na	L29		AarA	182	inactive	
			GlpG	na		0.6			chymo	10	na	
L2			AarA	74		393	L35		AarA	43	inactive	
	chymo		3	na	chymo	41			na			
	GlpG		na	1.3	GlpG	na			1.9			
L11		AarA	70	134	L41		AarA	47	inactive			
		chymo	2	na			chymo	103	na			
		GlpG	na	0.8			GlpG	na	0.8			
L14		AarA	29	nd*	L42		AarA	14	105			
		chymo	85	na			chymo	92	na			
		GlpG	na	inactive			GlpG	na	1.2			
L16		AarA	41	nd*	L44		AarA	6.8	95			
		chymo	36	na			chymo	1.43	na			
		GlpG	na	0.4			GlpG	na	inactive			
L18		AarA	26	nd*	L46		AarA	18.3	103			
		chymo	19	na			chymo	15	na			
		GlpG	na	1.3			GlpG	na	inactive			
L19		AarA	16	188	L47		AarA	85	nd*			
		chymo	0.3	na			chymo	16	na			
		GlpG	na	1.8			GlpG	na	1			
L25		AarA	20	nd*	L58		AarA	33	59			
		chymo	inactive	na			chymo	1.9	na			
		GlpG	na	1			GlpG	na	0.45			

<sup>1</sup>Endogenous GlpG activity in *E. coli* NR698 (see Methods). \*72–86% AarA activity at 100  $\mu$ M compound.

preferred GlpG over AarA (Table 1): potency was 67- to 302-fold greater on GlpG than on AarA for L2, L10, L11, L19, L42, and L58. This net preference is probably also true for L4, L16, L17, L18, L20, L25, L45, and L47 as AarA retained 71–86% of DMSO control activity at 100  $\mu$ M compound (Tables 1 and S3).

Although we cannot directly compare selectivity of compounds against GlpG and chymotrypsin, because they are assayed in two

different formats, we can deduce high selectivity for GlpG over chymotrypsin for compounds that already show selectivity for AarA in the fluorescent assay. Examples are compounds L25 and L42 where a net rhomboid preference over chymotrypsin was achieved, with a high selectivity for GlpG (Table 1).

To summarize our conclusions based on *in vitro* analysis of  $\beta$ -lactam inhibition of rhomboid activity, we found that (i) an

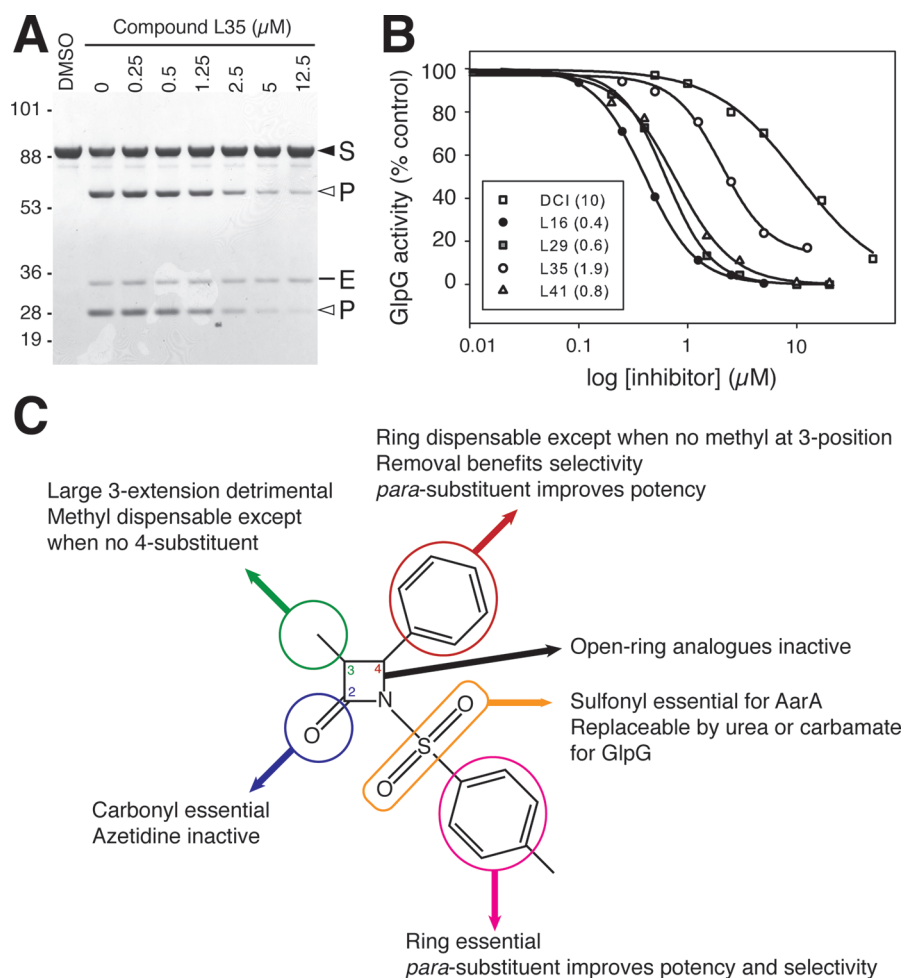


**Figure 4.** *In vitro* activity of  $\beta$ -lactams: high potency on GIpG and structure–activity relationship (SAR) against AarA and GIpG. (A) Typical gel showing  $\beta$ -lactam (L35) inhibiting the cleavage of Gurken chimeric substrate ( $3 \mu\text{M}$ ) by GIpG ( $320 \text{ nM}$ ). Enzyme (E), substrate (S), and product (P) bands are indicated. (B) Band intensity was quantified using Image J, and substrate conversion was expressed as % of DMSO control. The apparent  $\text{IC}_{50}$  values in brackets were determined by fitting the data to a 4-parameter logistic equation. (C) Diagram summarizing SAR results. Analogues based on the L1 skeleton were obtained by structural modifications of the encircled substituents.

intact  $\beta$ -lactam ring is required for activity, suggesting a mechanism of action involving nucleophilic attack at C-2; (ii)  $\beta$ -lactams showed greater potency on GIpG than on AarA; (iii) distinct structural modifications, summarized in Figure 4C, resulted in improved potency and differential selectivity between two bacterial rhomboids, as well as between rhomboid and chymotrypsin (Table 1). The fact that different  $\beta$ -lactams preferentially targeted AarA or GIpG is significant as it validates the concept of developing compounds to target specific rhomboids.

***In Vivo* Inhibition by  $\beta$ -Lactams.** Intramembrane proteases normally work in the lipid bilayer, but *in vitro* assays typically rely on detergent-solubilized enzyme activity. Are the  $\beta$ -lactam inhibitors we have identified effective *in vivo*? We tested whether any were able to inhibit endogenous GIpG in *E. coli*. To this end, the LacYTM2-containing fusion protein substrate of GIpG<sup>21</sup> was expressed in wild-type and GIpG-null strains of *E. coli*. Upon induction of substrate expression, only the wild-type strain was able to cleave LacYTM2, confirming that its processing is dependent on endogenous GIpG. Initial experiments indicated no inhibitory activity for the most potent  $\beta$ -lactams, and we reasoned that they might not be able to penetrate the bacterial outer membrane, which can form an impermeable barrier to

small molecules. We therefore assayed activity using an *E. coli* mutant strain defective in outer membrane biogenesis (NR698) that has been reported to display increased outer membrane permeability to small molecules.<sup>24</sup> Similar to the wild-type *E. coli*, NR698 was able to process the LacYTM2 substrate efficiently, and cleavage was completely abolished by *glpG* disruption (strain KS69) (Figure 5A). In this background, seven out of 16  $\beta$ -lactams inhibited endogenous GIpG, of which five (L16, L29, L35, L41, and L42) had an  $\text{EC}_{50}$  (defined as the concentration of the compound at which it exerted half of its maximal attainable effect<sup>25</sup>) between 5 and  $10 \mu\text{M}$  (Figure 5B, Table 1).

Finally, we also tested whether selected  $\beta$ -lactams showed inhibitory activity against a mammalian rhomboid. COS7 cells were transfected with C-terminally KDEL-tagged mouse rhomboid-2 (RHBDL2) and Gurken substrate. In this well-established assay,<sup>26</sup> the intracellular level of Gurken processing by RHBDL2 was assayed by comparing the ratio of product to substrate band intensity between the compound and solvent (DMSO) control. Out of 12  $\beta$ -lactams tested, some had an effect on protein expression but did not change the product to substrate band intensity ratio, whereas three compounds (L25, L29, and L58) reproducibly displayed detectable inhibition of RHBDL2 *in vivo*,

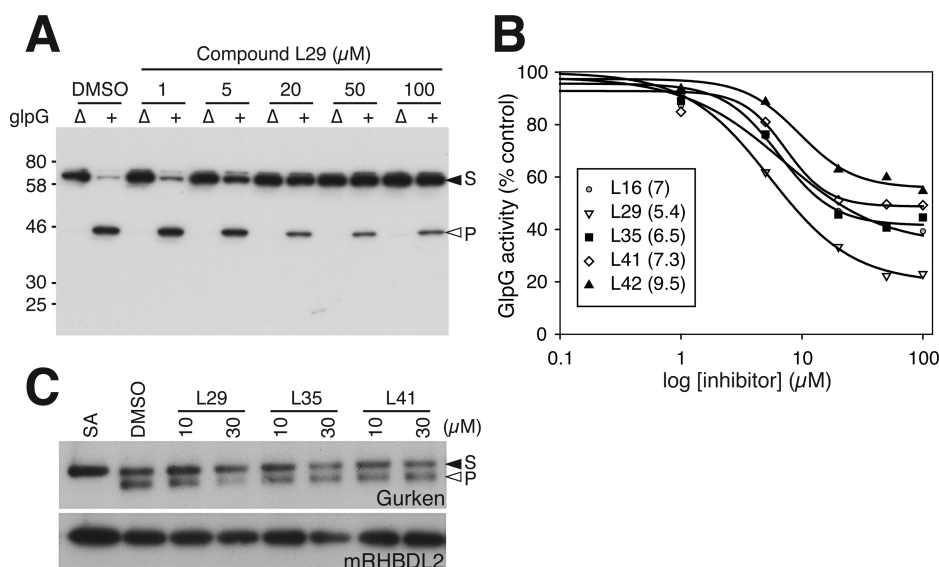


**Figure 5.** *In vivo* activity of  $\beta$ -lactams. (A) Inhibition of endogenous GlpG by L29 in *E. coli* NR698 carrying *imp4213* allele and a plasmid expressing the LacYTM2-based rhomboid substrate. Substrate (S) and product (P) were detected by Western blot with anti-Myc antibody, as described in Methods. The *E. coli* NR698 (+) or its  $\Delta$ glpG variant ( $\Delta$ ) were grown in the presence of inhibitors at a range of concentrations and 2% DMSO. (B) The *in vivo* EC<sub>50</sub> values ( $\mu$ M, in brackets) of selected  $\beta$ -lactams were obtained from band quantification performed as in Figure 4. Graph shows average data from three experiments, with standard errors up to 20%. (C) Mouse RHBDL2 was inhibited *in vivo* by L29, but not L35 and L41 (tested at 10 and 30  $\mu$ M). COS7 cells were transfected with mRHBDL2 and Gurken substrate. Western blot was probed with anti-FLAG (Gurken) or anti-HA (mRHBDL2) antibody. S and P represent the substrate and product band, respectively.

albeit at relatively modest levels. Notably, L29, the most potent inhibitor in bacteria, was also most potent against RHBDL2 (Figure 5C).

We conclude that selected monocyclic  $\beta$ -lactams not only are potent rhomboid inhibitors *in vitro* in the detergent micelle environment where our screen was performed but also can inhibit rhomboids in their native lipid membranes. Unlike isocoumarins, the best  $\beta$ -lactams are selective for rhomboids over chymotrypsin. Finally, our data show that monocyclic  $\beta$ -lactams can inhibit diverse prokaryotic and eukaryotic rhomboids and also that their selectivity is tunable by chemical modification.

**Mechanism of Action of  $\beta$ -Lactam Rhomboid Inhibitors.** Diverse  $\beta$ -lactams are inhibitors of several hydrolases, including some soluble serine proteases (reviewed in ref 23). However, rhomboids are evolutionarily unrelated to other proteases, and much remains unknown about their enzymatic activity, so it is impossible to predict with confidence the mechanism of their inhibition by the compounds we have identified. To begin to address this issue, we first tested whether inhibition was reversible, by following activity recovery after a rapid 100-fold dilution of the preincubated enzyme–inhibitor mixture into the reaction buffer and 30 min recovery period.<sup>27,28</sup> We tested four  $\beta$ -lactams (L19, L42, L43, and L45) with IC<sub>50</sub> < 20  $\mu$ M against AarA, along with DCI as a positive control. All behaved similarly to L42 (Figure 6A): we observed a partial and significant recovery of activity after 100-fold dilution of enzyme and inhibitor (20–35% activity of the DMSO control) but negligible recovery after 100-fold dilution of the enzyme maintaining the initial inhibitor concentration (2–7% the activity of DMSO control), indicative of partial or slow reversibility of inhibition. We also tested for time-dependence of inhibition, which is typical of irreversible inhibitors.<sup>23</sup> Consistent with this idea, prolonging the preincubation time of AarA and  $\beta$ -lactams led to progressively more potent

inhibitory effect (Figure 6B and data not shown). This point is important because it means that the apparent IC<sub>50</sub> values of the inhibitors will strongly depend on the length of time of preincubation with rhomboid (Figure S2). The IC<sub>50</sub> data reported in this paper all refer to 30 min preincubation.

Finally, to establish whether the inhibitors form covalent complexes with rhomboid, to assess the stoichiometry of such complexes, and to determine the possible specificity of this reaction for the catalytic serine, we used MALDI-TOF mass spectrometry. We analyzed the influence of two of the most potent  $\beta$ -lactam inhibitors of GlpG (L29 and L1) and an inactive  $\beta$ -lactam (L30) on the mass of purified full-length GlpG and its mutant form lacking the catalytic serine (S201A). In a proof-of-principle experiment we showed that 3-fold stoichiometric excess (100  $\mu$ M) of the known mechanism-based isocoumarin inhibitor JLK-6<sup>29</sup> generated a single adduct with wild-type GlpG but not with the S201A mutant (data not shown). Using the same experimental method, the  $\beta$ -lactams L29 and L1 caused a mass shift of the enzyme peak that was approximately equal to their molecular weight when incubated with wild-type GlpG but not with the catalytic serine mutant S201A (Figure 6C and not shown). Conversely, the  $\beta$ -lactam compound L30 that did not inhibit GlpG *in vitro* had no effect on the mass of either wild-type or catalytic serine mutant of GlpG (Figure 6C). These results demonstrate that monocyclic  $\beta$ -lactams inhibit rhomboid proteases by specific covalent binding to their catalytic serine. At present it is not clear whether the compounds L29 and L1 can also bind to the catalytic histidine: although a doubly bound adduct, with alkylation of the acyl enzyme intermediate through the active site His, has been described for some  $\beta$ -lactams,<sup>23</sup> the chemical structures of L29 and L1 suggest this to be unlikely. Moreover, the slow reversibility of inhibition indicated by the dilution assay rather suggests a single covalent link through the catalytic serine.<sup>23</sup> A definitive answer about the mechanism of



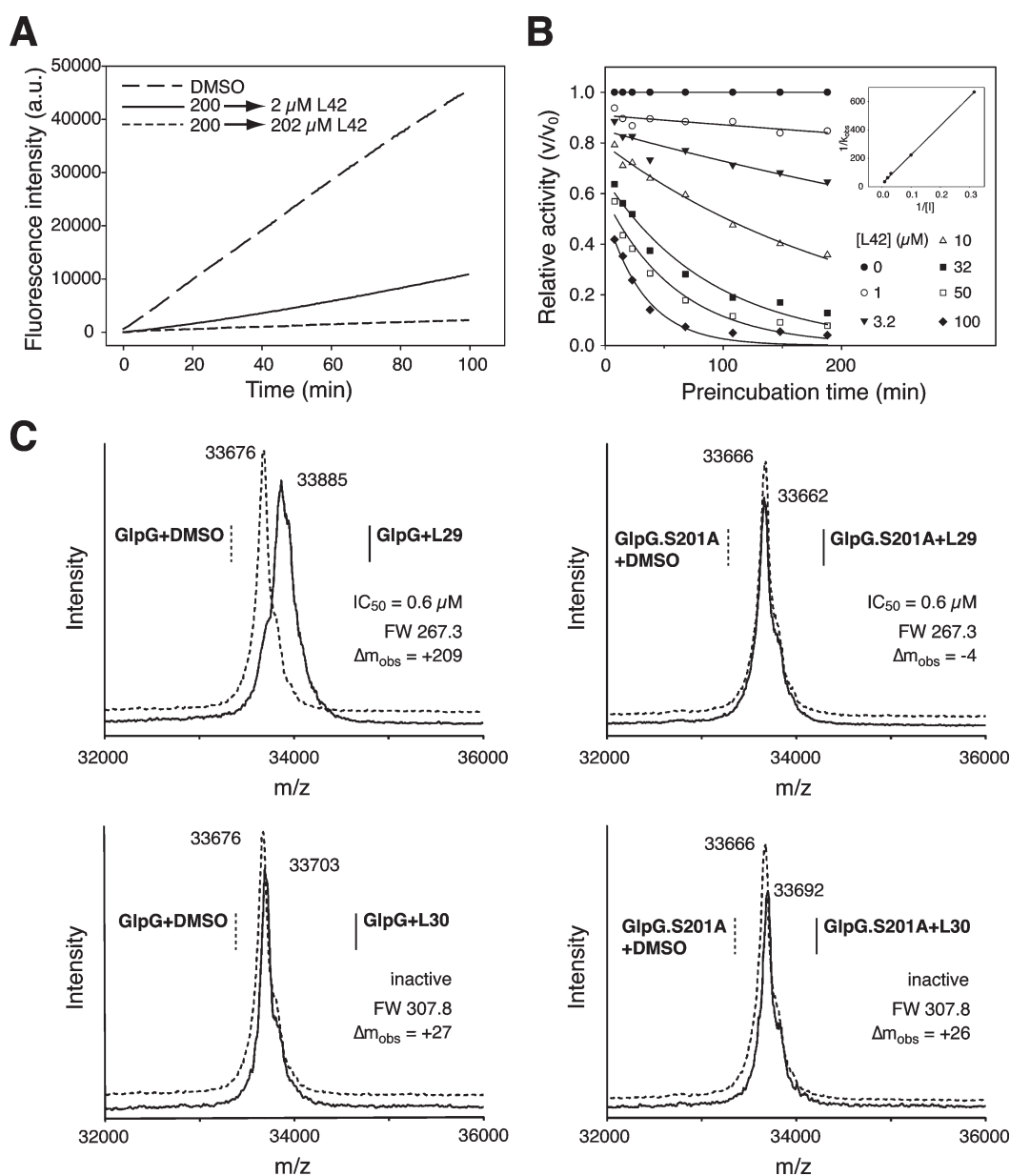


**Figure 6.** Mechanism of action of selected  $\beta$ -lactams. (A) Reversibility of L42 inhibition of AarA was tested using the 100-fold dilution technique described in Results. Enzyme was incubated with inhibitor or DMSO for 30 min pre- and postdilution (to 71 nM final concentration); residual activity was then assayed in the presence of 600 nM KSp21 substrate. (B) The L42 compound displays time-dependent inhibition of AarA. AarA (100 nM) was preincubated with 1–100  $\mu$ M L42 for varying times (8–188 min), after which activity was measured using 600 nM KSp21 fluorogenic substrate. Activities were expressed relative to the solvent (DMSO) control. The inset shows a plot of  $1/k_{obs}$  vs  $1/[\text{inhibitor concentration}]$ .<sup>31</sup> (C) The inhibitory monocyclic  $\beta$ -lactam L29 forms a 1:1 covalent complex with GlpG through its catalytic serine. GlpG or its S201A mutant (30  $\mu$ M) were incubated with the indicated compound (100  $\mu$ M) for 30 min at 25 °C, purified through a  $C_4$  ZipTip, and analyzed by MALDI-TOF mass spectrometry.

action will require more accurate mass data or a crystal structure of the enzyme–inhibitor complex.

**Concluding Remarks.** Intramembrane proteases like rhomboids are increasingly understood to control many important biological processes, but they are much less well characterized than most protease families. Until now, no rhomboid inhibitors have been identified, beyond a small number of broad-spectrum serine protease inhibitors, notably isocoumarins, which have weak inhibitory activity and high cytotoxicity. The monocyclic  $\beta$ -lactam inhibitors that we have now identified provide exciting starting points for further development of potent and specific rhomboid inhibitors. Moreover, since many  $\beta$ -lactams are already

used as pharmaceuticals, these molecules may provide valuable leads for future drug development.

## METHODS

**Materials.** Peptides were synthesized commercially, except for the MCA-DNP modified Gurken, which was made in-house. Fluorescent peptide KSp21 labeled with dark quencher QSY21 and Chromis-645-A-PDA fluorescent dye (50 mg) was synthesized by Cambridge Research Biochemicals (CRB). Dodecyl maltoside was from Glycon Biochemical or Anatrace. *E. coli* NR698 (MC4100 *imp4213*) was a generous gift from Dr. Tom Silhavy, Princeton University, NJ, USA.

**Recombinant Protein Expression and Purification.** Bacterial rhomboids (wild-type and its catalytic serine to alanine mutant) C-terminally His-tagged were expressed in *E. coli* C43(DE3),<sup>30</sup> isolated from membrane fraction, solubilized in dodecyl maltoside (DDM), and purified on a His-Pure Cobalt (ThermoScientific) affinity column. The column was washed with 10 mM imidazole in 20 mM Hepes-NaOH, 0.3 M NaCl, 10% (v/v) glycerol, 0.05% (w/v) DDM, pH 7.4. AarA and GlpG were eluted at 70 and 150 mM imidazole, respectively. Gurken or LacY derived chimeric substrates (MBP-TMD-Trx-His6<sup>19</sup>) were overexpressed in GlpG-deficient *E. coli* (MC4100 *glpG::tet*, strain KSS2), which had been generated by P1 phage mediated transduction of the *glpG::tet* allele from *E. coli* GW338<sup>21</sup> onto a fresh MC4100 background. Overexpressed chimeric substrates were isolated from the membrane fraction, solubilized in DDM, and purified on a His-Pure column (wash buffer, elution buffer and strip buffer at 25, 70, and 150 mM imidazole, respectively), except that Gurken TMD fusion was further purified on amylose resin (New England Biolabs).

**In Vitro Fluorescent Assay, HTS, and Counter-screen.** Rhomboid protease assay was performed at 24–25 °C in Nunc White 384-well plates (VWR) in a final reaction volume of 20  $\mu$ L. Each reaction contained the following final concentration of reagents: 25 mM Hepes pH 7.4, 5 mM EDTA, 5% (v/v) glycerol, 0.5% (w/v) DDM, 20% (v/v) DMSO, 100 nM rhomboid AarA or 37 nM chymotrypsin (Sigma), and 600 nM of rhomboid fluorescent peptide substrate. Importantly, increasing the DMSO concentration from 5% to 20% led to a linear increase in the cleavage rate of KSp21, suggesting that DMSO did not compromise AarA function in this concentration range. Using Biomek FX (Beckman-Coulter) robotics, 8  $\mu$ L of enzyme mix (reaction buffer, DDM, AarA, or enzyme buffer) was first added in each well, then 2  $\mu$ L of 200  $\mu$ M compound or DMSO only. All compounds were preincubated with the rhomboid enzyme for 30 min at 25 °C to accommodate any slow-binding effectors, and the reaction was started by the addition of 10  $\mu$ L of peptide mix (reaction buffer, DDM, DMSO, peptide) using a Flexdrop liquid dispenser (Perkin-Elmer). After 50–60 min, the reaction was stopped, while still in the linear phase, with 4  $\mu$ L of 1 M phosphoric acid pH 1.5 on a WellMate (ThermoScientific). Fluorescence intensity was detected using a Pherastar plate reader (BMG-Labtech) with excitation at 640 nm and emission at 680 nm. After screening 57,703 synthetic and natural compounds, we identified 162 hits, applying a cutoff at 80% (or 120%) activity of DMSO high control activity for hit confirmation and counter-screening. Counter-screen consisted of adding the compounds after the reaction was completed to identify compounds that interfered with the fluorescent signal, independent of rhomboid inhibition.

**Chemical Synthesis.** For variation of the bis-CF<sub>3</sub> aryl ring portion, the appropriate aniline was coupled with commercially available 3,3,3-trifluoro-2-(trifluoromethyl)propionic acid under nonbasic conditions. Noncommercial anilines were accessed by standard functional group transformations of nitro compounds, followed by reduction. Replacements for the bis-CF<sub>3</sub> group were prepared by coupling with the appropriate acid, followed by further transformations where necessary. Most  $\beta$ -lactams were prepared by N-sulfonylation of commercially available 4-phenylazetidine-2-one. Non-commercial C-4-substituted analogues were accessed by ring closure of the corresponding  $\beta$ -amino acids, followed by N-sulfonylation. Compounds with an amide at C-3 were prepared from N-protected DL-serine by ring closure of the N-methoxyamide, conversion to the N-sulfonyl  $\beta$ -lactam, deprotection of the C-3 amino group, and treatment with the acid chloride or acid under standard conditions. Open chain analogues were prepared by means of standard transformations on the corresponding amino acids.

**In Vitro Gel-Based Assay.** Activity of the best hits was assessed in an independent *in vitro* assay using purified recombinant protein substrates (MBP-TMD-Trx-His6, with LacY or Gurken TMD) followed by SDS-PAGE analysis of the cleavage products, as reported previously.<sup>19</sup> A typical 20  $\mu$ L reaction, run at 37 °C for 60–75 min, contained

25 mM Hepes-NaOH pH 7.4, 5 mM EDTA, 5% (v/v) glycerol, 0.05% (w/v) DDM, 0.4 M (for GlpG) or 0.1 M (for AarA) NaCl, 3  $\mu$ M chimeric protein substrate, 320 nM GlpG or 700 nM AarA, and 5% (v/v) DMSO. All compounds were preincubated with the enzymes for 30 min at 25 °C.

**In Vivo Assay in Bacteria.** The *glpG::tet* disruption allele from *E. coli* GW338<sup>21</sup> was transferred into *E. coli* NR698 genome using P1 phage transduction to generate strain KS69 ( $\Delta$ *glpG*), which was selected and maintained on 5  $\mu$ g/mL tetracycline. Both NR698 and KS69 were electroporated with pGW93 encoding  $\beta$ -lactamase-LacYTM2-MBP-His6-Myc chimera<sup>21</sup> and selected on 50  $\mu$ g/mL spectinomycin. NR698 and KS59 carrying pGW93 were grown overnight at 37 °C with 50  $\mu$ g/mL spectinomycin and 5  $\mu$ g/mL tetracycline. The next day, 1.5 mL of fresh LB medium was inoculated with 1/100 (NR698) or 1/33 (KS69) of overnight culture in the presence of spectinomycin. After ~2 h at 37 °C or when OD<sub>600 nm</sub> reached 0.3–0.4 absorbance unit, 150  $\mu$ L was transferred to clean tubes, and 3  $\mu$ L of DMSO or 1–100  $\mu$ M  $\beta$ -lactam was added (2% (v/v) DMSO throughout). After 15 min at RT, each tube was supplemented with 1 mM cAMP and 1 mM IPTG, and culture was maintained at 25 °C, 1200 rpm, for 1 h for recombinant protein expression.<sup>21</sup> Bacterial cells were collected by centrifugation, and pellets were dissolved in SDS-PAGE sample buffer. After electrophoresis on 4–20% Bis-Tris gradient gel (Invitrogen), samples were transferred to PVDF Immobilon-P membrane (Millipore), and protein loading and transfer efficiency were checked by Ponceau red staining. Myc-tagged proteins were visualized by anti-Myc primary (1:900 c-Myc (A-14):sc-789, Santa-Cruz Biotechnology, Inc.) and anti rabbit-HRP conjugate secondary antibodies and detected by enhanced chemiluminescence (GE Healthcare).

**In Vivo Assay in Mammalian Cells.** COS7 cells were transfected in 24-well plates with 20 ng of HA-tagged mouse RHBDL2-KDEL (RHBDL2) plasmid, 50 ng of FLAG-tagged Gurken substrate construct, and pcDNA3 vector up to a total amount of 200 ng DNA per well using Fugene6 (Roche). Inhibitors (dissolved in DMSO) were added 2 h post transfection to final concentrations of 10 and 30  $\mu$ M and 1% (v/v) DMSO. Twelve hours post transfection, cells were lysed in 1X SDS-PAGE sample buffer, and proteins were separated on a 4–20% Tris-glycine gradient gel (Invitrogen). Processing of Gurken by RHBDL2 was analyzed by Western Blot using HRP-conjugated anti-FLAG (Sigma) antibody for Gurken detection and HRP-conjugated anti-HA antibody (Covance) for RHBDL2 detection.

**Mass Spectrometry.** Purified full-length C-terminally His-tagged GlpG<sup>20</sup> and its active site mutant S201A (30  $\mu$ M) were incubated with 100  $\mu$ M inhibitor for 30 min at 25 °C in a buffer of pH 7.5 containing 20 mM HEPES, 0.05% (w/v) dodecylmaltoside, 100 mM NaCl, 10% (v/v) glycerol, and 5% (v/v) dimethylsulfoxide (DMSO). Samples were adjusted to 0.1% (v/v) trifluoroacetic acid (TFA) and purified using a C<sub>4</sub> ZipTip (Millipore) according to manufacturer's instructions, eluting into 5  $\mu$ L of 10 mg/mL  $\alpha$ -cyano-4-hydroxycinnamic acid (CHCA, Sigma) matrix dissolved in 50% (v/v) acetonitrile in water and 0.05% (v/v) TFA. The ZipTip eluates were spotted onto a thin layer of CHCA and immediately analyzed by MALDI-TOF mass spectrometry on a Voyager-DE PRO in linear positive mode with external mass calibration on bovine insulin, *E. coli* thioredoxin, and horse apomyoglobin (Calibration Mixture 3, Applied Biosystems).

## ■ ASSOCIATED CONTENT

Supporting Information. This material is available free of charge via the Internet at <http://pubs.acs.org>.

## ■ AUTHOR INFORMATION

### Corresponding Author

\*mf1@mrc-lmb.cam.ac.uk.

## Author Contributions

<sup>5</sup>These authors contributed equally to this work

## ACKNOWLEDGMENT

We thank our colleagues Debbie Taylor for valuable strategic input, Simon Osborne for expert chemical advice, David Whalley and Puneet Khurana for help with the HTS robotics, David Owen for peptide synthesis and Elaine Stephens for advice on mass spectrometry. We are also grateful to Yoshinori Akiyama (Kyoto) for plasmids and *glpG* knock-out strains of *E. coli* and to Tom Silhavy (Princeton) for *E. coli* strain NR698. O.A.P. was partly funded by the MRC Technology Development Gap Fund. K.S. acknowledges support from a Marie Curie Intra-European Fellowship, EMBO Long-Term Fellowship, and Medical Research Council UK Career Development Fellowship.

## REFERENCES

- (1) Rawson, R. B., Zelenski, N. G., Nijhawan, D., Ye, J., Sakai, J., Hasan, M. T., Chang, T. Y., Brown, M. S., and Goldstein, J. L. (1997) Complementation cloning of S2P, a gene encoding a putative metalloprotease required for intramembrane cleavage of SREBPs. *Mol. Cell* 1, 47–57.
- (2) De Strooper, B., Saftig, P., Craessaerts, K., Vanderstichele, H., Guhde, G., Annaert, W., Von Figura, K., and Van Leuven, F. (1998) Deficiency of presenilin-1 inhibits the normal cleavage of amyloid precursor protein. *Nature* 391, 387–390.
- (3) Weihofen, A., Binns, K., Lemberg, M. K., Ashman, K., and Martoglio, B. (2002) Identification of signal peptide peptidase, a presenilin-type aspartic protease. *Science* 296, 2215–2218.
- (4) Urban, S., Lee, J. R., and Freeman, M. (2001) Drosophila rhomboid-1 defines a family of putative intramembrane serine proteases. *Cell* 107, 173–182.
- (5) Urban, S., Lee, J. R., and Freeman, M. (2002) A family of Rhomboid intramembrane proteases activates all Drosophila membrane-tethered EGF ligands. *EMBO J.* 21, 4277–4286.
- (6) Lee, J. R., Urban, S., Garvey, C. F., and Freeman, M. (2001) Regulated intracellular ligand transport and proteolysis control EGF signal activation in Drosophila. *Cell* 107, 161–171.
- (7) Herlan, M., Vogel, F., Bornhovd, C., Neupert, W., and Reichert, A. S. (2003) Processing of Mgm1 by the rhomboid-type protease Pcp1 is required for maintenance of mitochondrial morphology and of mitochondrial DNA. *J. Biol. Chem.* 278, 27781–27788.
- (8) McQuibban, G. A., Saurya, S., and Freeman, M. (2003) Mitochondrial membrane remodeling regulated by a conserved rhomboid protease. *Nature* 423, 537–541.
- (9) McQuibban, G. A., Lee, J. R., Zheng, L., Juusola, M., and Freeman, M. (2006) Normal mitochondrial dynamics requires rhomboid-7 and affects Drosophila lifespan and neuronal function. *Curr. Biol.* 16, 982–989.
- (10) O'Donnell, R. A., Hackett, F., Howell, S. A., Treeck, M., Struck, N., Krnajska, Z., Withers-Martinez, C., Gilberger, T. W., and Blackman, M. J. (2006) Intramembrane proteolysis mediates shedding of a key adhesin during erythrocyte invasion by the malaria parasite. *J. Cell Biol.* 174, 1023–1033.
- (11) Baker, R. P., Wijetilaka, R., and Urban, S. (2006) Two Plasmodium rhomboid proteases preferentially cleave different adhesins implicated in all invasive stages of malaria. *PLoS Pathog.* 2, e113.
- (12) Srinivasan, P., Coppens, I., and Jacobs-Lorena, M. (2009) Distinct roles of Plasmodium rhomboid 1 in parasite development and malaria pathogenesis. *PLoS Pathog.* 5, e1000262.
- (13) Stevenson, L. G., Strisovsky, K., Clemmer, K. M., Bhatt, S., Freeman, M., and Rather, P. N. (2007) Rhomboid protease AarA mediates quorum-sensing in *Providencia stuartii* by activating TatA of the twin-arginine translocase. *Proc. Natl. Acad. Sci. U.S.A.* 104, 1003–1008.
- (14) Wang, Y., Zhang, Y., and Ha, Y. (2006) Crystal structure of a rhomboid family intramembrane protease. *Nature* 444, 179–180.
- (15) Urban, S., and Wolfe, M. S. (2005) Reconstitution of intramembrane proteolysis in vitro reveals that pure rhomboid is sufficient for catalysis and specificity. *Proc. Natl. Acad. Sci. U.S.A.* 102, 1883–1888.
- (16) Baxt, L. A., Rastew, E., Bracha, R., Mirelman, D., and Singh, U. (2010) Downregulation of an Entamoeba histolytica rhomboid protease reveals roles in regulating parasite adhesion and phagocytosis. *Eukaryotic Cell* 9, 1283–1293.
- (17) Freeman, M. (2008) Rhomboid proteases and their biological functions. *Annu. Rev. Genet.* 42, 191–210.
- (18) Urban, S. (2009) Making the cut: central roles of intramembrane proteolysis in pathogenic microorganisms. *Nat. Rev. Microbiol.* 7, 411–423.
- (19) Strisovsky, K., Sharpe, H. J., and Freeman, M. (2009) Sequence-specific intramembrane proteolysis: identification of a recognition motif in rhomboid substrates. *Mol. Cell* 36, 1048–1059.
- (20) Lemberg, M. K., Menendez, J., Misik, A., Garcia, M., Koth, C. M., and Freeman, M. (2005) Mechanism of intramembrane proteolysis investigated with purified rhomboid proteases. *EMBO J.* 24, 464–472.
- (21) Maegawa, S., Ito, K., and Akiyama, Y. (2005) Proteolytic action of GlpG, a rhomboid protease in the Escherichia coli cytoplasmic membrane. *Biochemistry* 44, 13543–13552.
- (22) Zhang, J. H., Chung, T. D., and Oldenburg, K. R. (1999) A simple statistical parameter for use in evaluation and validation of high throughput screening assays. *J. Biomol. Screening* 4, 67–73.
- (23) Powers, J. C., Asgian, J. L., Ekici, O. D., and James, K. E. (2002) Irreversible inhibitors of serine, cysteine, and threonine proteases. *Chem. Rev.* 102, 4639–4750.
- (24) Ruiz, N., Falcone, B., Kahne, D., and Silhavy, T. J. (2005) Chemical conditionality: a genetic strategy to probe organelle assembly. *Cell* 121, 307–317.
- (25) Neubig, R. R., Spedding, M., Kenakin, T., and Christopoulos, A. (2003) International Union of Pharmacology Committee on Receptor Nomenclature and Drug Classification. XXXVIII. Update on terms and symbols in quantitative pharmacology. *Pharmacol. Rev.* 55, 597–606.
- (26) Urban, S., Schlieper, D., and Freeman, M. (2002) Conservation of intramembrane proteolytic activity and substrate specificity in prokaryotic and eukaryotic rhomboids. *Curr. Biol.* 12, 1507–1512.
- (27) Harper, J. W., Hemmi, K., and Powers, J. C. (1985) Reaction of serine proteases with substituted isocoumarins: discovery of 3,4-dichloroisocoumarin, a new general mechanism based serine protease inhibitor. *Biochemistry* 24, 1831–1841.
- (28) Harper, J. W., and Powers, J. C. (1985) Reaction of serine proteases with substituted 3-alkoxy-4-chloroisocoumarins and 3-alkoxy-7-amino-4-chloroisocoumarins: new reactive mechanism-based inhibitors. *Biochemistry* 24, 7200–7213.
- (29) Vinothkumar, K. R., Strisovsky, K., Andreeva, A., Christova, Y., Verhelst, S., and Freeman, M. (2010) The structural basis for catalysis and substrate specificity of a rhomboid protease. *EMBO J.* 29, 3797–3809.
- (30) Miroux, B., and Walker, J. E. (1996) Over-production of proteins in Escherichia coli: mutant hosts that allow synthesis of some membrane proteins and globular proteins at high levels. *J. Mol. Biol.* 260, 289–298.
- (31) Kitz, R., and Wilson, I. B. (1962) Esters of methanesulfonic acid as irreversible inhibitors of acetylcholinesterase. *J. Biol. Chem.* 237, 3245–3249.